

Methylation by Set9 modulates FoxO3 stability and transcriptional activity

Daniel R. Calnan^{1,2}, Ashley E. Webb², Jamie L. White², Timothy R. Stowe^{1,2,3}, Tapasree Goswami⁴, Xiaobing Shi³, Alexandra Espejo⁵, Mark T. Bedford⁵, Or Gozani³, Steven P. Gygi⁴, and Anne Brunet^{1,2}

¹ Cancer Biology Program, Stanford University, Stanford, CA 94305

² Department of Genetics, Stanford University, Stanford, CA 94305

³ Department of Biology, Stanford University, Stanford, CA 94305

⁴ Department of Cell Biology, Harvard Medical School, Boston, MA 02115

⁵ Science Park-Research Division, the University of Texas M. D. Anderson Cancer Center, Smithville, TX 78957

Key words: longevity, FOXO transcription factors, methyltransferase, Set9, aging

Received: 7/5/12; Accepted: 7/19/12; Published: 7/21/12

Correspondence to: Anne Brunet, PhD; E-mail: anne.brunet@stanford.edu

Copyright: © Calnan et al. This is an open-access article distributed under the terms of the Creative Commons Attribution License, which permits unrestricted use, distribution, and reproduction in any medium, provided the original author and source are credited

Abstract: The FoxO family of transcription factors plays an important role in longevity and tumor suppression by regulating the expression of a wide range of target genes. FoxO3 has recently been found to be associated with extreme longevity in humans and to regulate the homeostasis of adult stem cell pools in mammals, which may contribute to longevity. The activity of FoxO3 is controlled by a variety of post-translational modifications that have been proposed to form a 'code' affecting FoxO3 subcellular localization, DNA binding ability, protein-protein interactions and protein stability. Lysine methylation is a crucial post-translational modification on histones that regulates chromatin accessibility and is a key part of the 'histone code'. However, whether lysine methylation plays a role in modulating FoxO3 activity has never been examined. Here we show that the methyltransferase Set9 directly methylates FoxO3 in vitro and in cells. Using a combination of tandem mass spectrometry and methyl-specific antibodies, we find that Set9 methylates FoxO3 at a single residue, lysine 271, a site previously known to be deacetylated by Sirt1. Methylation of FoxO3 by Set9 decreases FoxO3 protein stability, while moderately increasing FoxO3 transcriptional activity. The modulation of FoxO3 stability and activity by methylation may be critical for fine-tuning cellular responses to stress stimuli, which may in turn affect FoxO3's ability to promote tumor suppression and longevity.

INTRODUCTION

FoxO transcription factors mediate longevity downstream of the insulin pathway in worms and flies [1-5]. In mammals, the role of FoxO factors in longevity has not been investigated yet, but mice with mutations in the insulin or IGF-1 receptors are long-lived [6, 7]. In addition, recent genetic studies on long-lived humans have shown that single nucleotide polymorphisms (SNPs) in the FoxO3 gene, one of the four human FoxO family members, are closely linked to extreme longevity and the reduction in age-related diseases [8-12]. These studies are consistent with the

notion that mammalian FoxO3 may also be involved in regulating longevity. Importantly, FoxO transcription factors also act as tumor suppressors in mammals [13]. Indeed, mice in which the FoxO1, FoxO3, and FoxO4 genes are conditionally deleted in the adults develop thymic lymphomas and hemangiomas [14]. In humans, inactivation of FoxO3 correlates with poor prognosis in estrogen-dependent breast cancer [15, 16], illustrating the conserved role of the FoxO family in tumor suppression.

In mammalian cells, FoxO factors act as potent transcriptional activators that upregulate the expression

of programs of genes involved in stress resistance, cell cycle arrest, differentiation, apoptosis, autophagy, and metabolism [17-30]. Recent evidence indicates that FoxO factors, and in particular FoxO3, is important for the maintenance of adult neural and hematopoietic stem cells [31-35]. However, much remains unknown about how FoxO transcription factors integrate extracellular stimuli to regulate different programs of gene expression and cellular responses that ultimately lead to lifespan extension and tumor suppression.

FoxO transcription factors are regulated by a wide array of external stimuli, ranging from insulin and growth factors to oxidative and nutrient stresses [36], as well as a variety of chemical activators such as LY294002 [37] and hypomethylating agents such as azacitidine and decitabine [38]. The principal mode of regulation of FoxO factors is via post-translational modifications (PTMs). Phosphorylation by the insulin-activated protein kinases Akt and SGK at three conserved sites on FoxO factors leads to the sequestration of FoxO in the cytoplasm, thereby preventing FoxO factors from transactivating their target genes [18, 39-42]. Phosphorylation of FoxO factors in response to insulin pathway stimulation and to cytokines also promotes the degradation of FoxO factors by the ubiquitin-proteasome pathway [15, 43-46].

FoxO factors are post-translationally modified at a number of lysine residues by ubiquitination and acetylation. For example, FoxO1 is polyubiquitinated by the SCF^{skp2} complex [46], and FoxO3 is polyubiquitinated by MDM2 and Skp-2 [47, 48], prior to degradation. FoxO factors can also be mono-ubiquitinated, which promotes FoxO nuclear translocation and regulates FoxO transcriptional activity [49, 50]. Acetylation/deacetylation of FoxO factors at a number of lysine residues also regulates FoxO subcellular localization, DNA binding capacity and transcriptional activity towards specific target genes [51-61]. The large number and diversity of PTMs on FoxO factors have lead us to hypothesize that these PTMs form a 'FoxO code' that could regulate several aspects of FoxO activity [62].

Methylation of lysine residues is a critical PTM for the regulation of histone proteins in chromatin [63]. There are about 50 lysine methyltransferases in mammals [64, 65]. The Su(var), Enhancer of zeste, and Trithorax [28]-domain containing lysine methyltransferases are conserved throughout species and catalyze a variety of histone methylations that are critical in regulating chromatin structure. Interestingly, some lysine methyltransferases can also methylate non-histone proteins. For example, Set9 (also known as Set7/9 and

KMT7) was first identified as a mono-methyltransferase for lysine 4 in Histone H3 (H3K4) [66], but Set9 also methylates several non-histone proteins, including transcription factors (RelA (p65), p53, ER α), enzymes (DNMT1, PCAF), and transcription-initiation proteins (TAF10) [67-73]. Set9 methylation has been shown to affect the protein stability of Rel, p53, ER α and DNMT1 [67-69, 73, 74], and to alter the recruitment of transcription factors and transcriptional machinery such as RelA and TAF10 to different promoters [71, 72]. These observations suggest that Set9 has a complex role beyond chromatin regulation.

The importance of Set9 in the organism is underscored by the observation that half of the Set9 knockout mice die prior to birth [75]. Mouse embryonic fibroblasts (MEFs) from Set9 heterozygous and null mice are more susceptible to transformation than wildtype MEFs, suggesting that Set9, like FoxO3, acts as a tumor suppressor [75]. This observation, coupled with the role of Set9 in a variety of cellular processes also regulated by FoxO3, including cell cycle arrest [69, 75] and apoptosis [69], and the activation of Set9 by stress stimuli [69, 74], raised the possibility of a connection between Set9 and FoxO3.

Here we find that the lysine methyltransferase Set9 methylates FoxO3 directly *in vitro* and in cells. We identify a single lysine residue methylated by Set9 on FoxO3. This residue is important in modulating the transcriptional activity of FoxO3 and its stability. In addition to uncovering a novel non-histone substrate for Set9, our study identifies lysine methylation as an additional post-translational modification of FoxO3 that is likely part of the 'code' that modulates FoxO3's activity in response to environmental stimuli. Our findings further our understanding of the regulation of a critical transcription factor involved in longevity and cancer, and expand our knowledge of the role of Set9 in cells.

RESULTS

FoxO3 is Methylated by Set9 *in Vitro*

Among the four FoxO family members, FoxO3 is the isoform that has been associated with human longevity [8-11], breast cancer suppression in humans [15, 16], and in the maintenance of adult hematopoietic and neural stem cells [31, 34], a potentially important process in maintaining health late in life. Thus, we focused on FoxO3, and screened for lysine methyltransferases that could methylate the N-terminal or C-terminal portions of FoxO3 in an *in vitro* methylation assay (Fig. 1A, B). We found that among

eight methyltransferases, only Set9, a member of the Set domain-containing lysine methyltransferase family, methylated the N-terminal domain of FoxO3 (Fig. 1A). We confirmed that full-length FoxO3 was methylated by Set9, and that only the N-terminal portion (1-300) of FoxO3 was methylated by Set9 (Fig. 1A-C). These results indicate that FoxO3 is a substrate of Set9 *in vitro* and that the site of methylation is located between amino acids 1-300 of FoxO3.

FoxO3 is Methylated by Set9 at Lysine 271 *in Vitro*

To identify the site(s) of methylation of FoxO3 by Set9, we analyzed the peptides generated by enzymatic digest of full-length FoxO3 that had been methylated by Set9 *in vitro* using tandem mass spectrometry (Fig. 2A). This tandem mass spectrometry analysis revealed that 9

lysines of FoxO3 were methylated *in vitro* by Set9: K46, K149, K230, K262, K269, K270, K271, K290, K419. With the exception of K419, all the sites of methylation identified by mass spectrometry were located between amino acids 1-300 of FoxO3, consistent with our observation that this portion of FoxO3 was the one methylated by Set9 (see Fig. 1). Based on the number of peptides identified, mono-methylation of K271 was the most prominent post-translational modification of FoxO3 by Set9 (Fig. 2A, peptides in bold). K290 was also found on multiple peptides to be mono- or di-methylated. However, because Set9 has been reported to be capable of only mono-methylating its substrates due to the structure of the active site [76], it is possible that the di-methylation is an artefact of tandem mass spectrometry.

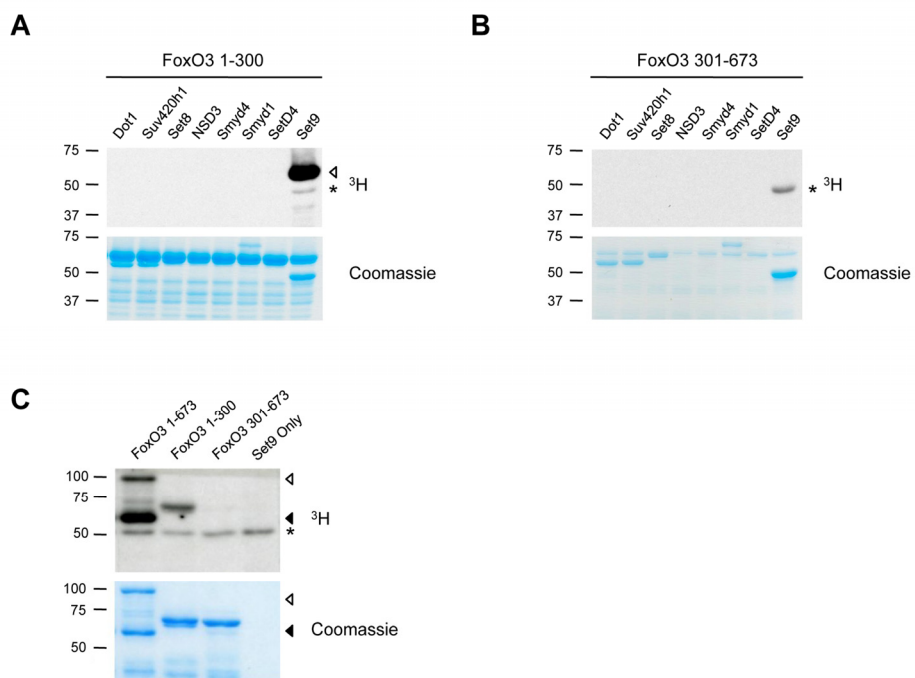


Figure 1. FoxO3 is methylated by Set9 *in vitro*. (A) *In vitro* methylation of the N-terminal portion of FoxO3 (amino acids 1-300) by 8 different methyltransferases. \blacktriangleleft : FoxO3 methylated by Set9, *: Set9 auto-methylation. (B) *In vitro* methylation of the C-terminal portion of FoxO3 (amino acids 301-673) by 8 different methyltransferases. *: Set9 auto-methylation. (C) Methylation of the full-length FoxO3 protein by Set9. \blacktriangleleft : full-length FoxO3, \blacktriangleleft : FoxO3 degradation product, *: Set9 auto-methylation.

A

Peptide	Lysine	Methylation	Lysine	Methylation
RPELQASPAK*PSGETAADSMIPEEEEDDEDDEDGGRA	46	1		
RPELQASPAK*PSGETAADSMIPEEEEDDEDDEDGGRA	46	2		
RK*CSSRRNAWGNLSYADLITRA	149	1		
RK*CSSRRNAWGNLSYADLITRA	149	1		
RK*CSSRRNAWGNLSYADLITRA	149	2		
RVQNEGTGK*SSWWIINPDGGKS	230	2		
KYTKSRSRGRAAK*K	262	2	269	2
KK*KAALQTAPESADDSPSQLSKW	270	1		
KK*ALQQTAPESADDSPSQLSKW	271	1		
KK*ALQQTAPESADDSPSQLSKW	271	1	290	1
KK*ALQQTAPESADDSPSQLSKW	271	1	290	2
KK*ALQQTAPESADDSPSQLSKW	271	1	290	2
KK*ALQQTAPESADDSPSQLSKW	271	1	290	2
KK*ALQQTAPESADDSPSQLSKW	271	1	290	2
KK*ALQQTAPESADDSPSQLSKW	271	3		
KAALQTAPESADDSPSQLSKW	290	1		
KAALQTAPESADDSPSQLSKW	290	2		
KAALQTAPESADDSPSQLSKW	290	2		
KKAALQTAPESADDSPSQLSKW	290	2		
RSSSFPTTK*G	419	2		

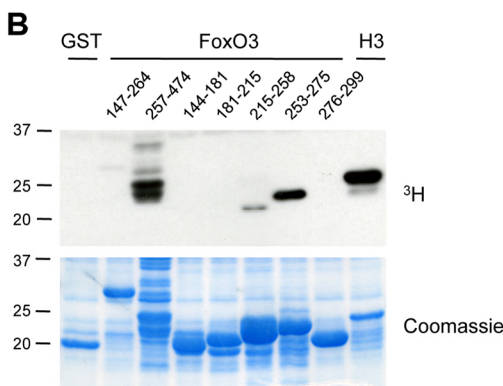
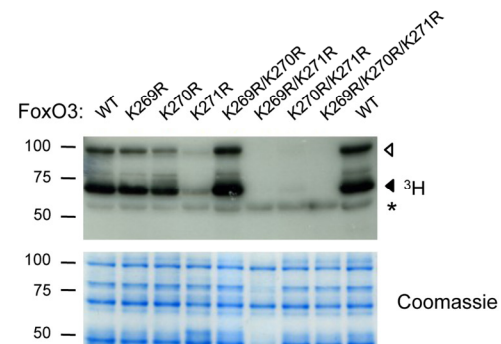
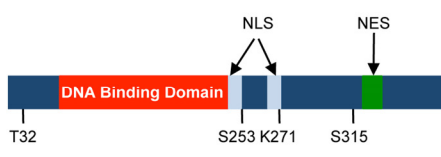
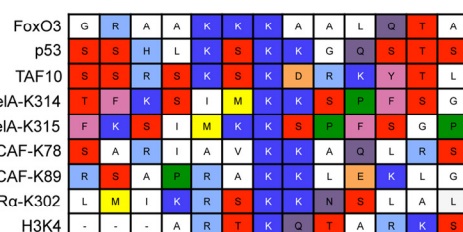
B**C****D****E**

Figure 2. Set9 mono-methylates FoxO3 at K271 in vitro. (A) Tandem mass spectrometry on *in vitro* methylated full-length FoxO3. Peptides containing methylated lysines are shown and the number of the methylated lysine in the human FoxO3 amino acid sequence is indicated. Methylated lysines are followed by an *. The type of methylation (mono-, di-, or tri-) is indicated by 1, 2, or 3, respectively. (B) Deletion analysis to map the region of FoxO3 containing the methylation site. *In vitro* methylation of overlapping fragments spanning the N-terminal domain of FoxO3 by Set9. (C) Methylation of FoxO3 WT or mutants of specific lysine residues. Each mutant was made in the context of the GST-FoxO3 protein (amino acid 1-525). ▲: FoxO3, ▲: FoxO3 degradation product, *: Set9 auto-methylation. (D) Location of K271 compared to other domains and PTMs of FoxO3. Listed are Akt phosphorylation sites (T32, S253, and S315), DNA binding domain, and NLS and NES (nuclear export sequence). K271 is the final amino acid in the second part of the bipartite FoxO3 NLS. (E) Alignment of the region surrounding the residues methylated by Set9 in a series of known Set9 substrates.

To identify in an independent manner the main site(s) of FoxO3 methylated by Set9, we used a deletion approach. We found that the regions between amino acids 257-474 and 253-275 were heavily methylated by Set9, whereas the region between 215-258 only displayed trace levels of methylation by Set9 (Fig. 2B). There are five lysine residues in the portion of FoxO3 comprised between amino acids 257-275, four of which that have also been identified by tandem mass spectrometry as methylated by Set9 (K262, K269, K270, K271). In contrast, the regions between amino acids 144-215, and 276-299 were not methylated at all by Set9 (Fig. 2B), suggesting that K149 and K290 are not major methylation sites in FoxO3, even though they were identified by mass spectrometry.

To identify the main residue of FoxO3 methylated by Set9, we generated point mutants of FoxO3 for which K269, K270, or K271 were replaced by an arginine, either individually or concomitantly. We compared the *in vitro* methylation by Set9 of wildtype (WT) FoxO3 with that of each FoxO3 mutant. The FoxO3 mutant in which lysine 271 was replaced by an arginine (K271R) was the only mutant that showed a significant decrease in methylation by Set9 (Fig. 2C). In addition, the double mutants that contained K271R (K269R/K271R and K270R/K271R) were no longer methylated by Set9, whereas the double K269R/K270R mutant showed levels of methylation by Set9 that were similar to that of WT FoxO3 (Fig. 2C). K262R and K290R mutants did not display lower levels of methylation as compared to wild type FoxO3 (data not shown). Taken together, these results indicate that lysine 271, a residue located in the second half of the bipartite nuclear localization sequence (NLS) of FoxO3 [77], is the primary methylation site on FoxO3 by Set9 *in vitro* (Fig. 2D).

To determine if the amino acids surrounding K271 formed a potential consensus sequence for Set9 methylation, we aligned a 13 amino acid region surrounding this site in FoxO3 with regions of similar length surrounding the Set9-methylated lysine residues in previously identified substrates (Fig. 2E). This alignment did not reveal a clear consensus sequence for Set9 methylated sites, but it suggested that Set9 requires positively charged residues (K or R) in the vicinity of the methylated lysine (Fig. 2E).

FoxO3 is the FoxO Family Member Most Strongly Methylated by Set9

We next asked if Set9 also methylated other mammalian FoxO family members (human FoxO1, human FoxO4, and mouse FoxO6), as well as FoxO orthologs in other species (DAF-16, the worm FoxO). While we do see

methylation of other mammalian FoxO family members (most notably a fragment of mouse FoxO6) as well as worm ortholog DAF-16, surprisingly, FoxO3 was the only protein in the FoxO family that was robustly methylated by Set9 under the conditions used (Fig. 3A).

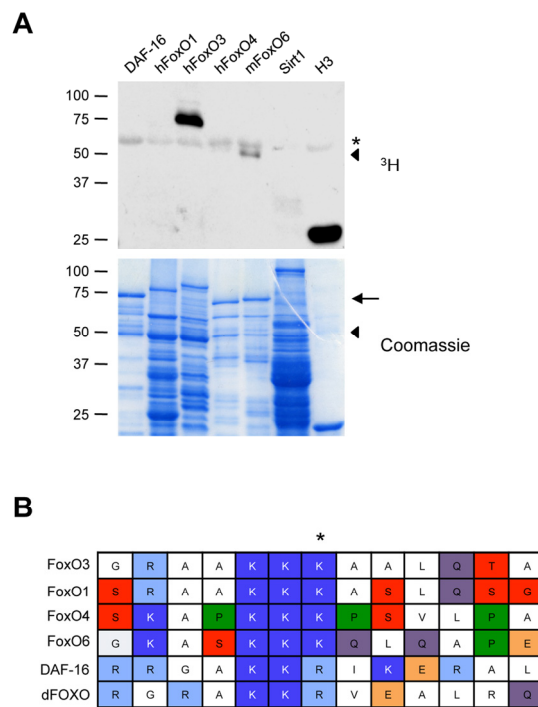


Figure 3. Set9 preferentially methylates FoxO3 among FoxO family members. (A) *In vitro* methylation of different mammalian FoxO family members or FoxO orthologs. The FoxO1, FoxO3 and FoxO4 constructs were generated from the human sequence, whereas the FoxO6 construct was generated from the mouse sequence. ▲: FoxO6 degradation product, ←: full-length FoxO6, *: Set9 auto-methylation. (B) Alignment of the region of FoxO3 surrounding K271 to that of other mammalian FoxO family members and FoxO orthologs.

To determine if there was a particularity in FoxO3 sequence underlying the specificity of Set9 towards FoxO3, we aligned the region surrounding FoxO3 K271 with that of other mammalian and non-mammalian FoxO family members. This analysis revealed that the lysine residues corresponding to K271 are conserved in all mammalian FoxO family members (Fig. 3B), suggesting that there are other parameters, such as secondary structure, that may influence the relative specificity of Set9 for FoxO3.

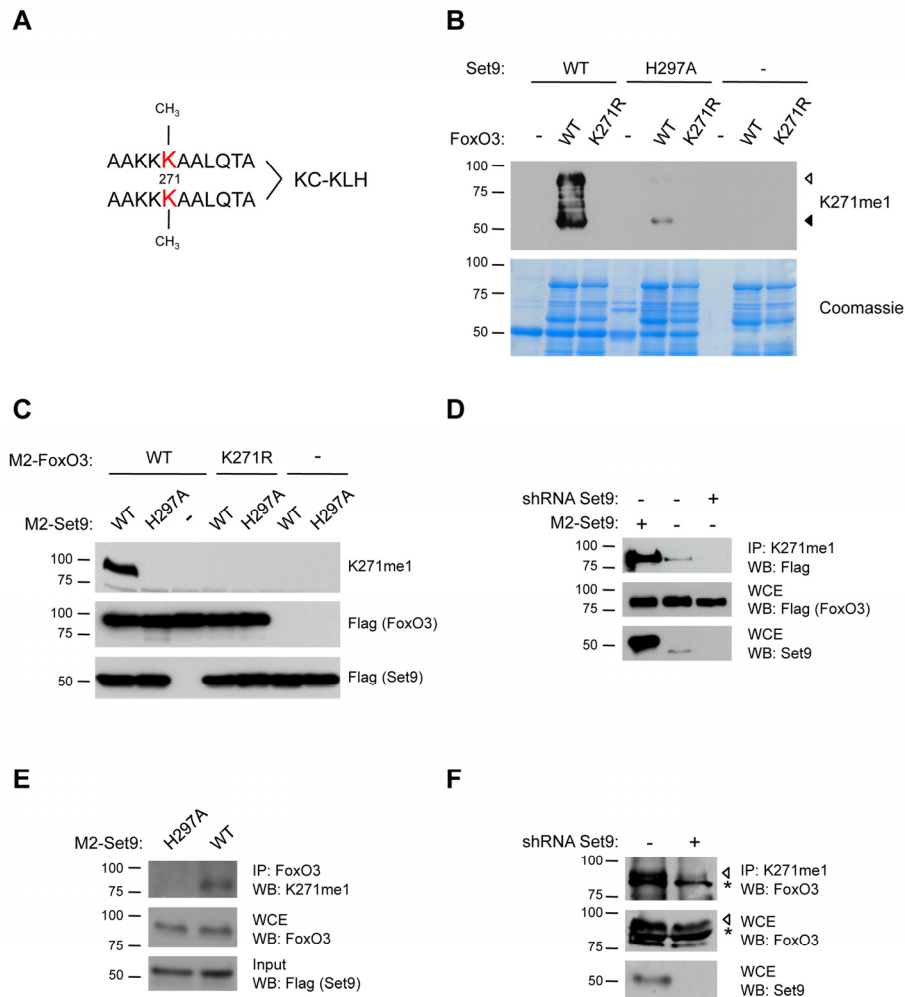


Figure 4. FoxO3 is methylated at K271 in cells. (A) Scheme for generation of K271me1 antibody. A branched mono-methylated 11 amino acid peptide surrounding FoxO3 K271 was used as the epitope. (B) The K271me1 antibody is specific to FoxO3 that has been methylated at K271 in *in vitro* methylation assays. *In vitro* methylation assays were conducted with cold SAM and analyzed by western-blot with the K271me1 antibody [33]. Coomassie staining was used to show equal levels of FoxO3 and Set9 were used in each condition (bottom). ▲: FoxO3, ▲: FoxO3 degradation product. (C) The K271me1 antibody is specific to FoxO3 K271 methylation in cells. Flag-FoxO3 and Flag-Set9 (WT or H297A methyltransferase-deficient mutant) were co-expressed in 293T cells, and FoxO3 methylation was analyzed by western-blot with the K271me1 antibody. (D) Endogenous Set9 methylates ectopically expressed FoxO3. The methylated form of FoxO3 was immunoprecipitated from a 293T cell line with a stable knock-down of Set9 using the K271me1 antibody and the IP eluates were analyzed by western-blot with the Flag antibody. (E) Endogenous FoxO3 is methylated by overexpressed Set9. 293T cells were transfected with Flag-Set9, and FoxO3 was immunoprecipitated with an antibody to total FoxO3. The IP eluates were analyzed by western-blot with the K271me1 antibody. (F) Endogenous FoxO3 is methylated by endogenous Set9. Methylated FoxO3 was immunoprecipitated from the stable Set9 shRNA cell line used in (D) using the K271me1 antibody. The IP eluate was analyzed by western-blot with an antibody to total FoxO3. ▲: FoxO3, *: non-specific band.

FoxO3 is Methylated by Set9 at K271 in Human Cells

To investigate whether FoxO3 is methylated by Set9 in mammalian cells, we generated an antibody specifically directed to the mono-methylated lysine 271 of FoxO3

(K271me1). As an epitope, we used a branched peptide that contains two mono-methylated epitopes per molecule (Fig. 4A). To test the specificity of this antibody to methylated FoxO3, we performed an *in vitro* methylation assay with wild type (WT) FoxO3 or

the FoxO3 K271R mutant as substrates, and either WT Set9 or a methyltransferase-deficient version of Set9 (H297A) as the enzyme [66]. The K271me1 antibody recognized only WT FoxO3 that was incubated with WT Set9, and did not recognize FoxO3 K271R mutant (Fig. 4B). The K271me1 antibody did not recognize FoxO3 in the presence of the methyltransferase-deficient mutant of Set9, confirming the specificity of this antibody (Fig. 4B). There was a minor signal from a degradation fragment of FoxO3 in the presence of the Set9 methyltransferase-deficient mutant, which might be due to the fact that this mutant is not completely deficient for methyltransferase activity *in vitro*. Together, these results indicate that the antibody is specific for methylation of K271 on FoxO3 *in vitro*.

To test whether FoxO3 was methylated by Set9 in mammalian cells, we co-transfected human 293T cells with constructs encoding Flag-tagged versions of FoxO3 and Set9, and examined FoxO3 methylation by western-blot with the K271me1 antibody. We found that the expression of Flag-Set9 led to an increased methylation of WT FoxO3 (Fig. 4C). In contrast, when the methyltransferase-deficient Set9 mutant (H297A) was co-expressed with FoxO3, FoxO3 was no longer recognized by the K271me1 antibody (Fig. 4C). Furthermore, a mutant of FoxO3 containing a point mutation for the methylation site identified *in vitro* (K271R) was not recognized by the antibody to K271me1, even when co-expressed with WT Set9 (Fig. 4C). Taken together, these results confirm that the antibody to K271me1 we generated is specific, and indicate that overexpressed Set9 can methylate FoxO3 at lysine 271 in mammalian cells.

To examine if endogenous Set9 is necessary for FoxO3 methylation in 293T cells, we generated a stable cell line in which an shRNA against Set9 was introduced by viral transduction. The efficiency of Set9 knock-down in this cell line was confirmed by western-blot with an antibody to endogenous Set9 (Fig. 4D). To assess the methylation level of FoxO3 in the Set9 knock-down stable cell line, we immunoprecipitated Flag-FoxO3 in this cell line or in control cells and performed western-blot with the K271me1 antibody. We found that this antibody recognized a band at the molecular weight of FoxO3 in cells overexpressing FoxO3 alone in the control cell line and that this signal was reduced in the stable cell line with a Set9 shRNA knock-down (Fig. 4D). These results indicate that endogenous Set9 is necessary for the methylation of overexpressed Flag-FoxO3.

Conversely, to determine if endogenous FoxO3 is methylated by Set9 in mammalian cells, we

overexpressed WT Set9 or the methyltransferase-deficient mutant of Set9 (H297A) in 293T cells and immunoprecipitated endogenous FoxO3 from these cells with an antibody to FoxO3 (Fig. 4E). We then assessed if endogenous FoxO3 was methylated using the K271me1 antibody in western-blot experiments. This antibody detected a band at the appropriate molecular weight for FoxO3 when FoxO3 was immunoprecipitated from cells expressing WT Set9, but not from cells expressing the inactive H297A mutant of Set9 (Fig. 4E). These data indicate that endogenous FoxO3 is methylated by overexpressed Set9.

Finally, to test if endogenous FoxO3 is methylated in cells by endogenous Set9, we used the stable cell line with Set9 knock-down. Protein lysates from these cells and control cells were subjected to immunoprecipitation with the K271me1 FoxO3 antibody and analyzed by western-blot using the antibody to total FoxO3 (Fig. 4F). These experiments revealed a band that corresponds to FoxO3 in the control cell line and the intensity of this band was reduced in the cell line with knocked down Set9 (Fig. 4F), indicating that endogenous FoxO3 is methylated by endogenous Set9 in cells.

Taken together, these experiments indicate that FoxO3 is methylated by Set9 in the human 293T cell line, and that Set9 is necessary and sufficient for lysine 271 mono-methylation on FoxO3.

The Methylated Form of FoxO3 Has Similar Localization to Total FoxO3

To examine the localization of methylated FoxO3 in cells, we conducted immunofluorescence experiments on NIH 3T3 cells expressing FoxO3-GFP using the K271me1 antibody. When Set9 was co-transfected with FoxO3-GFP, the K271me1 antibody detected a signal in FoxO3-GFP expressing cells (Fig. 5A). The signal from the K271me1 was significantly reduced when either the methyltransferase-deficient mutant of Set9 (H297A) was expressed or when cells expressed the K271R mutant of FoxO3, indicating that the immunofluorescence signal was specific for Set9 methylation of K271 (Fig. 5A). The localization of the methylated form of FoxO3 overlapped with that of total FoxO3, suggesting that methylation does not influence FoxO3 subcellular localization.

To further test whether methylation by Set9 affects FoxO3 localization, we transfected a human glioblastoma cell line (U87) with FoxO3-GFP and either Set9 WT or the methyltransferase-deficient mutant of Set9 (H297A). We chose the U87 cell line because these cells have high transfection efficiency and a relatively flat morphology,

which is helpful to assess FoxO3 subcellular localization. FoxO3-GFP localization was scored ‘nuclear’ if the nucleus was clearly identifiable in the GFP channel, ‘cytoplasmic’ if the exclusion from the nucleus was visible in the GFP channel, and ‘ubiquitous’ if neither of these conditions was met. As expected, a constitutively active version of the protein kinase Akt significantly

increased the cyto-plasmic localization of FoxO3-GFP (Fig. 5B). In contrast, WT Set9 expression did not significantly affect the localization of FoxO3-GFP, as compared to expression of the methyltransferase-defective H297A Set9 mutant or the empty vector (Fig. 5B). Thus, methylation by Set9 does not appear to affect FoxO3 subcellular localization in U87 cells.

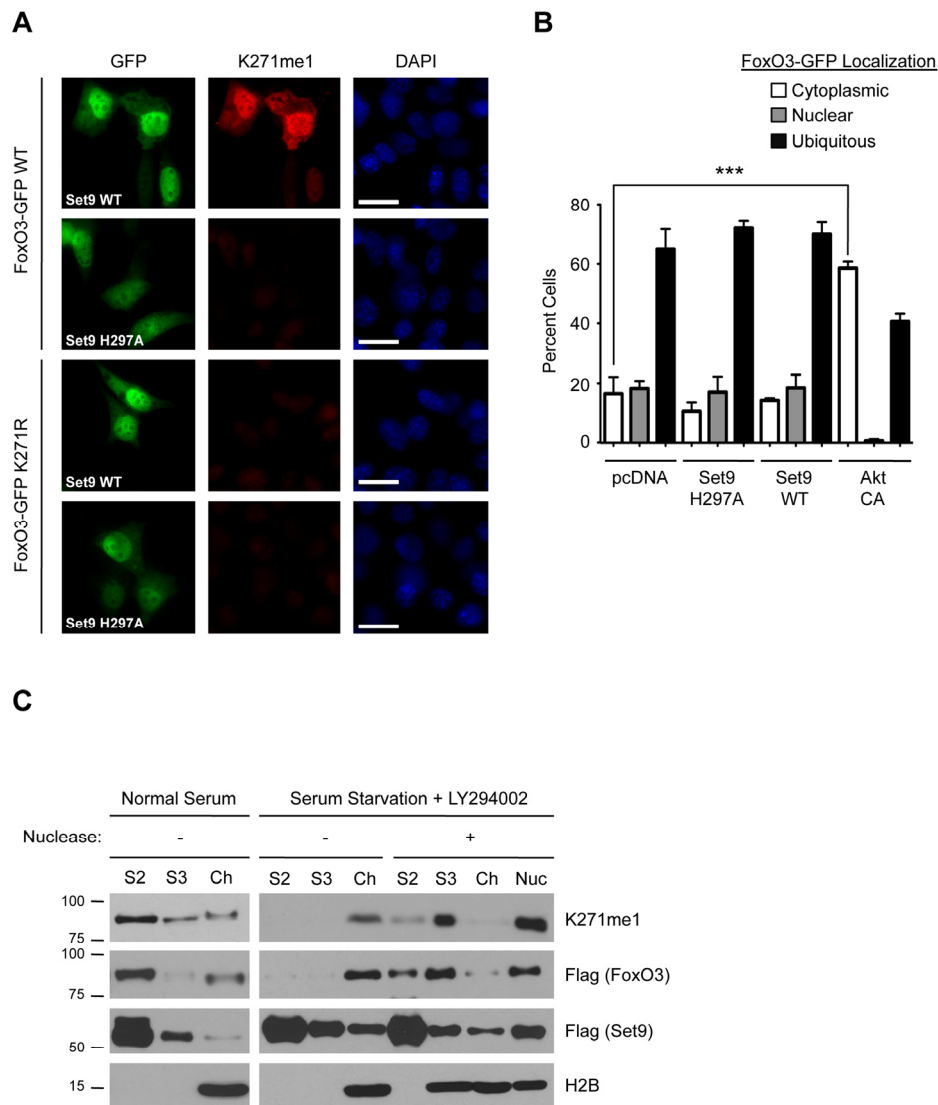
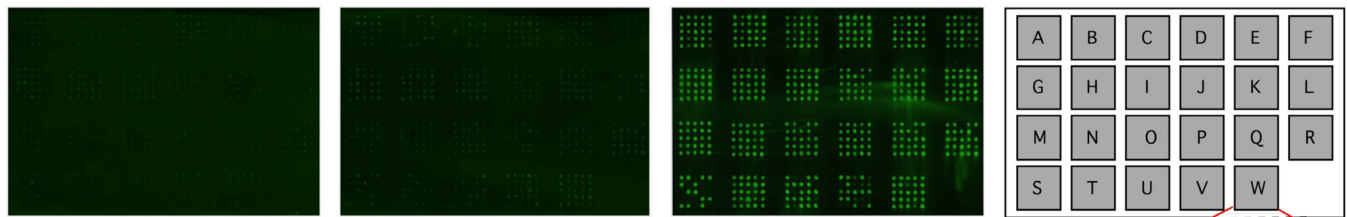


Figure 5. The methylated form of FoxO3 has similar localization properties to FoxO3. (A) Immunofluorescence in NIH 3T3 cells expressing FoxO3-GFP (green), using the K271me1 antibody (red). Nuclei were stained with DAPI (blue). White bar: 10 mm. (B) Quantification of FoxO3-GFP localization in U87 cells. Cells were co-transfected with FoxO3-GFP and empty vector (pcDNA), Set9 (WT or H297A), or a constitutively active version of Akt as a positive control (Akt CA). Localization was scored as ‘nuclear’, ‘cytoplasmic’ or ‘ubiquitous’. The data represent the mean and SEM from 3 independent experiments. In each experiment, at least 200 cells per condition were scored. *** p<0.001, one way ANOVA, Bonferroni post-test (C) Chromatin fractionation of 293T cells co-transfected with Flag-FoxO3 and Flag-Set9. Cells were grown in media with 10% FBS (Normal Serum) or in media without serum in the presence of 20 μ M LY294002 (Serum Starvation+LY294002) and then fractionated. A subset of the fractions was treated with micrococcal nuclease to digest the chromatin. Presence of chromatin-bound proteins in fractions was assessed by western-blot with antibodies to the core nucleosome histone H2B (H2B). S2: detergent lysis, S3: hypotonic lysis fraction, Ch: chromatin fraction, Nuc: supernatant from nuclease digest of chromatin.



K271 mono-methylated peptide

Unmethylated peptide

GST-Alexa Fluor 555

TUDOR	TUDOR	TUDOR	TUDOR	MBT-TUDOR	W4D0
A1 TDRD1(1)(NP_112568)	B1 EBNA-2Co-A(NP_055205)	C1 ESET(NP_036564)	D1 Lin9 TDR(b)(AAH65302)	E1 L13MBT(NP_056293)	F1 WDR5(d)(NP_543124)
A2 TDRD1(1)(NP_112568)	B2 Ret-bp1(AAB28543)	C2 CG1-72(NP_057102)	D2 LBR TDR(NP_919424)	E2 SCML1(NP_057413)	F2 WDR9(NM_018963)
A3 TDRD2(NP_006853)	B3 M6G1AH(0013)	C3 FX(AAH67272)	D3 LBR211(NP_919424)	E3 SCML2(AAH64617)	F3 WDR10(NP_057319)
A4 TDRD3(9)(NP_05833)	B4 STK31(Q9BXU1)	C4 PHF2(NP_057520)	D4 SP30(c)(Q75940)	E4 SCML1(AAH21252)	F4 TDR11(1)(AAH64544)
A5 TDRD4-1(Q9NUY9)	B5 S3BP1(1)(NP_005648)	C5 Pombe 1(CAA22823)	D5 JUN128 WT(I)(NP_055830)	E5 LML2(Q969R5)	F5 RbaB-6(G)(Q740729)
A6 TDRD4-2(Q9NUY9)	B6 S3BP1(1)(NP_005648)	C6 Pombe 2(CAB39904)	D6 Lin9 RPTD(AAH65302)	E6 KIAA1617(XP_166140)	F6 RbaB-8(G)(Q74262)
A7 TDRD4-3(Q9NUY9)	B7 S3BP1(2)(NP_005648)	C7 Colon 1(AAC18034)	D7 Colon Short-1-(AAC18034)	E7 PHF20 MBT(NP_057520)	F7 EDDINM_152991
A8 TDRD5(Q8NAT2)	B8 Anchor (NP_03479)	C8 Colon 2(AAC18034)	D8 ARH4A (e)(NM_002892)	E8 CG1-72-MBT(NP_057102)	F8 HIRAC(R456503)
A9 TDRD7-1(NP_055105)	B9 BNP(NP_055830)	C9 Colon 2(AAC18034)	D9 SETB1 (e)(NM_012432)	E9 PHF20 MBT-TDR(NP_057520)	F9 WDR11(NP_057319)
A10 TDRD7-3(NP_055105)	B10 C2NP(NP_055876)	C10 JMD2A-1(NP_055478)	D10 SND1 (e)(NM_014390)	E11 p5mbt HIS(a)(NP_609606)	F10 p5mbt50(i)(AAF78464)
A11 TDRD7-1-3(NP_055105)	B11 RBP1 (NP_112739)	C11 JMD2A-2(NP_055478)	D11 STK31(e)(NM_031414)	E12 L3(MBT)(NP_056293)	F11 DDB2(NM_000107)
A12 Tudor (NP_64591)	B12 SMN (NP_075012)	C12 JMD2A1-2(NP_055478)	D12 LTR Like Spindlin1	E13 MBT2(NM_153252)	F12 BWP03(NM_153252)
PhD	PhD	PIN +	BROMO	BROMO	SANT / TSN
G1 BPTF(P+B)(BA89208)	H1 Dnm1-3a-His(g)	I1 JMD2A2Phd+2Tudor(NP_055478)	J1 GON3(NP28230)	K1 TIF1 alpha(AAD17258)	L1 MP1-like(XP_379909)
G2 ING2(e)(AAH50003)	H2 Dnm2-3b-His(g)	I2 JMD2BPhd(NP_055478)	J2 TAF1-D1(NP_620278)	K2 KAP-1(AA837341)	L2 MT1A(Q13330)
G3 PHF2(NP_055383)	H3 Dm3T3L N-term-His	I3 M6G1Tudor-Phd(AAH0013)	J3 TAF1-D2(NP_620278)	K3 P300(NP_004571)	L3 N-Cor2(Q9Y618)
G4 PHF8(CA42860)	H4 Trim24-Brd-Phd (u)	I4 MYST4Pd-Phd(AAH48199)	J4 P/CAF (S71788)	K4 HD9R_1-2(Q9NS16)	L4 N-Cor2-1(Q9Y618)
G5 DAT1(CA95708)	H5 ING3	I5 NSD1-Phd+PWPW(P96L73)	J5 SP140(NP_009168)	K5 HD9R_1(Q9NS16)	L5 N-Cor2-2(Q9Y618)
G6 Rag2(NM_000536)	H6 ING4	I6 WHC1Phd+PWPW(P97887)	J6 SNF2 beta(G45252)	K6 HD9R_2(Q9NS16)	L6 N-Cor1(NP_006302)
G7 PCCX1(NP_055408)	H7 INGS	I7 PRKCB1Phd+BRD+PWPW(P99U14)	J7 SMAP(NP_899203)	K7 BA2NP_075381	L7 RERE(AAH62342)
G8 P300(P+B)(NM_001429)	H8 PHD _TIF1A(e) (O15164)	I8 BS69Phd+BRD(AAH2586)	J8 BAF180_1-2(NP_060635)	K8 BDT1-2(AAH62700)	L8 ADA2-SANT(NP_001479)
G9 PHF20 (PHD(NP_057520)	H9 TR66(e) (O15016)	I9 ATRX	J9 BAF180_3-4(NP_060635)	K9 BDT1 (AAH62700)	L9 Zootin Rel.(XP_168590)
G10 PHD FHS	H10 BRPF1(e) (P55201)	I10 RAL1	J10 BAF180_3-4(NP_060635)	K10 BDT2 (AAH62700)	L10 TSN (t)
G11 PHD FHS	H11 MLL4(e) (Q9UNM6)	I11 Ba2b1/WSTF	J11 BAF180_5-6(NP_060635)	K11 BDT2 1SANT/SWIRM	L11 TSN m5(t)
G12 PHD CHD5 (1-2)	H12 MIF2(e) (Q9Y485)	I12 CBP	J12 CBP	K12 BDT2 m6(t)	L12 TSN m6(t)
CHROMO	CHROMO	CHROMO / BMR / MRG	PWWP	PWWP / CW	ANK
M1 TIP60(h)(AA818236)	N1 Mi-2(b)(CAA60384)	O1 CBX3(e) (NM_016587)	P1 BBRF1(AAH53851)	Q1 PWWP_PKB(CB1(e)) (NM_183047)	R1 BARD1 (NP_000456)
M2 CHD2(h)(AA887382)	N2 H1 (AAH54973)	O2 CBX2(e) (NM_005205)	P2 BS69(AAH12586)	Q2 PWWP_HDGR3(e) (NM_016073)	R2 G9a delta (CAAA9491)
M3 CHD3(h)(AAH38596)	N3 H3 (AAH54973)	O3 CBX3(e) (NM_016587)	P3 DSMBT3(NP_094BC3)	Q3 PWWP_DSMBT3(e) (NM_175629)	R3 hG9a#3(CAA49491)
M4 MPBP9(h)	N4 Me3-Lksh(e)(AAQ34949)	O4 CBX8(e) (NM_066464)	P4 HD9R_1(Q9NS16)	Q4 PWWP_HD9R1(Q9NS16)	R4 N-Cor1MT1
M5 SMARCC2(h)(AAH26222)	N5 SUV39H(h)(AA892224)	O5 BRK_SMC4(e) (NM_03070)	P5 HRP-3(BAA90477)	Q5 CW3(AAH02725)	R5 NSD3
M6 MRG15(t)(AA29872)	N6 CBX1(h)(AA21972)	O6 BRK_SMC4(e) (NM_030702)	P6 MSH6(P52701)	Q6 CW4(CAD2056)	R6 MMPP (NP_09990)
M7 RBBP1(h)(AA41239)	N7 H1 (beta)(h)(P23197)	O7 BRK_CHD6(e) (NM_032221)	P7 NSD1(Q96L73)	Q7 CW5(AAH04985)	R7 RFX delta(CAG33262)
M8 PC2((h)(AA80718)	N8 CDY1(h)(AA22735)	O8 BRK_CHD6(e) (NM_017780)	P8 WHSC1-1(NP_579877)	Q8 CW6(P_087384)	R8 RFX3(CAG33262)
M9 CHD5(h)(AAH5495)	N9 CBX4(e) (NM_0036555)	O9 BRK_CHD6(e) (NM_017784)	P9 PSP1(e) (NM_032222)	Q9 FATM14	R9 Anc1(AA54554)
M10 CHD5(h)(AAK56405)	N10 CBX4(e) (NM_0036555)	O10 BRK_CHD6(e) (NM_017784)	P10 BRD1(e) (NM_014577)	Q10 TAF10 TAFH	R10 S3BP2(AAH58918)
M11 CHD7 (1-2)(AB037837)	N11 CBX7(e) (NM_175709)	O11 CBX5(e) (NM_012117)	P11 ZCPW1 (e)(AL136735)	Q11 TULP1	R11 Notch (NP_060087)
M12 CBX6/NPCD(BC012111)	N12 CBX5(e) (NM_012117)	O12 CBP	P12 MBDS (e)(NM_018328)		
FHA/KH/BRCT(t)	BRCT(t)	Others	Other	Others	
S1 RAD 53 H4A2(j)	T1 BRC41	U1 NO66 M1 (p)	V1 POZ Zbtb4(m)	W1 FG_Nup 116(y)	
S2 RAD 53 FA1(j)	T2 53BP1	U2 NO66M2 (p)	V2 POZ KA150(m)	W2 FG_Nup 42(y)	
S3 MDC1 FA (i)	T3 Crb2	U3 NO66 M5 (p)	V3 His-MBD1(n)	W3 FG_Nup2(y)	
S4 KIF14 (h)-168(k)	T4 Torsin1-6	U4 NO66 M6 (p)	V4 MBD2(n)	W4 FG_Nup 120(y)	
S5 CH2 FA(h)	T5 Rad4 I, II	U5 NO66 M22 (q)	V5 MBD3(n)	W5 X_Arry_ARV(x)	
S6 GAM 68 KH(t)	T6 Rad4 III, IV	U6 His-Dnka 343(q)	V6 McP2(n)	W6 X_Arry_Beta(x)	
S7 QKI(KH(t))	T7 Ect2	U7 SWIRM_KIAA01915(BAB7808)	V7 SMFBT1 L(L)0	W7 X_Arry_Delta(x)	
S8 BRCT_FCP1	T8 LigaseIV	U8 SWIRM_KIAA0601(CAB72299)	V8 SMFBT4 x-MBT(t)	W8 Lap2 Lem (v)	
S9 BRCT Bard1	T9 MDC1	U9 SWIRM_ADA2(NP_001479)	V9 WD40 Tap5	W9 Lap2 Lem Mut(v)	
S10 BRCT TDT	T10 REV1	U10 SWIRM_SMC2(e) (NM_033222)	V10 WD40 CS5	W10 Lap2 Lem like7(v)	
	T11 REV1	U11 SWIRM_SMC1(e) (NM_014577)	V11 SWIRM_SMC1(e) (NM_014577)	W11 SWIRM_SMC1(e) (NM_014577)	
	T12 DNA LIGASE II	U12 SWIRM_SMC1(e) (NM_014577)	V12 PHD_ZPF(s)	W12 Plantagenet_FXR1(e)(NM_005087)	

Figure 6. The methylated K271 peptide does not bind to known methyl-lysine binding domains. Twenty-one amino acid peptides surrounding K271, either mono-methylated (left) or unmethylated (right) were incubated with potential methyl-lysine and acetyl-lysine binding domains on a protein array. GST-Alexa Fluor 555 is used as a positive control. A detailed description of the binding domains present on the protein array is provided in the lower panels.

The Methylated Form of FoxO3 Associates with Chromatin Upon FoxO3 Activation

We next sought to determine if methyl-FoxO3 is associated with the chromatin. We co-expressed Flag-FoxO3 with Flag-Set9 in 293T cells under basal conditions or under conditions that are known to activate FoxO3 (serum starvation in the presence of the PI3K inhibitor LY294002 [18]), and we performed cellular fractionation experiments to separate the non-soluble chromatin fraction (Ch) from the soluble, non-chromatin fractions (S2 and S3). Under basal conditions,

we observed that total FoxO3 is primarily present in the non-chromatin fraction (S2), with very little FoxO3 in the chromatin fraction (Fig. 5C). Western-blotting with the K271me1 antibody revealed that the distribution of the methylated form of FoxO3 was similar to that of total FoxO3, with most of the signal present in the S2 fraction. Upon conditions that activate FoxO3, we found that total FoxO3 relocalized to the chromatin fraction (Fig. 5C). The methylated form of FoxO3 also relocalized to the chromatin fraction. Nuclease treatment of the chromatin fraction resulted in a shift in the distribution of FoxO3 from the chromatin fraction to

the S3 fraction, indicating that FoxO3, and methyl-FoxO3, were bound to the chromatin and not to membrane proteins or other cell components in the chromatin pellet. These results indicate that FoxO3 relocates to the chromatin fraction upon activation and that the methylated form of FoxO3 is also found at the chromatin.

Methylation of FoxO3 Does Not Cause Increased Association with Methyl-Lysine Binding Proteins

Because methyl-FoxO3 is localized to the chromatin under after serum starvation and LY294002 treatment, we asked if binding proteins that are known to bind to methylated histones could interact with the methylated fraction of FoxO3 (Fig. 6). We used a protein array that contained 265 domains found in chromatin associated proteins [78], many of which are known methyl-lysine binding domains (including TUDOR domains, PhD domains, and chromo-domains) or acetyl-lysine binding domains (including bromo-domains, for a complete list see Fig. 6, lower panels). We probed this protein array with a biotinylated 21 amino acid peptide surrounding K271 of FoxO3 either non-methylated (unmethylated peptide) or mono-methylated at K271 (K271 mono-methylated peptide). Peptide binding to the methyl-lysine binding domains on the array was assessed by immunofluorescence with antibodies to the biotin moiety. We did not observe binding of the K271 mono-methylated peptide for any of the domains present on the protein array (Fig. 6). These data suggest that mono-methylation of FoxO3 does not induce the binding to any of these chromatin-binding domains, although we cannot exclude that in the context of the whole protein, methylated FoxO3 may bind to chromatin-binding proteins that 'read' histone marks.

Methylation by Set9 Decreases the Stability of the FoxO3 protein

Methylation by Set9 has been shown to affect the protein stability of RelA, Era, DNMT1 and p53 [67-69, 73, 74]. To test the possibility that Set9 methylation affected FoxO3 protein stability, we co-transfected wild type FoxO3 together with either WT Set9 or the methyltransferase-deficient mutant of Set9 (H297A) in 293T cells. We then treated the cells with a series of different proteasome inhibitors: ALLN, Proteasome Inhibitor 1 (PSI-1), and MG132. The levels of c-Jun, a protein known to be degraded via a proteasome dependent pathway was increased upon treatment with proteasome inhibitors, indicating that these inhibitors were indeed effective at blocking the proteasome (Fig. 7A). We found that treatment of cells with proteasome inhibitors caused both total FoxO3 and methyl-FoxO3

levels to increase. Interestingly, densitometry measurements of the relative amount of FoxO3 levels normalized to β -actin levels showed an increase in the methyl-FoxO3 levels compared to total levels of FoxO3 when cells were treated with proteasome inhibitors (Fig. 7A-B). Although the effects of MG132 on FoxO3 were not statistically significant, there was a trend towards increased relative levels of methylated FoxO3 in the presence of MG132 (Fig. 7B). Together, these results suggest that the methylated form of FoxO3 is less stable than the non-methylated version of FoxO3.

FoxO3 K271R Mutant is More Stable than Wild Type FoxO3

To further explore whether methylation at lysine 271 might control the stability of FoxO3, we transfected 293T cells with WT FoxO3 or the K271R mutant form of FoxO3 together with WT or H297A Set9, and treated cells with cycloheximide to block de novo translation. Interestingly, we found that FoxO3 K271R was more stable than WT FoxO3 (Fig. 7C-D). We also found that WT FoxO3 was slightly less stable when co-expressed with WT Set9 as compared to H297A Set9 (Fig. 7C-D). These results suggest that methylation of lysine 271 is important for regulating the stability of FoxO3 in cells.

Set9 Leads to a Modest Increase in Nuclear FoxO3 Transcriptional Activity

To test if Set9 affected FoxO3 transcriptional activity, we co-transfected 293T cells with Set9 (WT or methyltransferase-deficient mutant [H297A]), together with FoxO3 (WT, K271R, a constitutively nuclear mutant in which all three Akt phosphorylation sites have been converted to alanines [TM], and the combined mutant TM K271R), and with a luciferase reporter construct that contained 6 FoxO DNA binding elements (6xDBE) (Fig. 7E). Co-expressing Set9 WT together with the constitutively nuclear form of FoxO3 (FoxO3 TM) led to a modest, but significant increase in the luciferase reporter activity compared to co-expression of the methyltransferase-deficient form of Set9 and FoxO3 TM (Fig. 7E). This result suggests that Set9 increases FoxO3 transcriptional activity. The TM K271R mutant of FoxO3 had an increased luciferase activity compared to TM FoxO3, probably because mutating K271 increased stability of the TM mutant (Fig. 7E). However, Set9 did not further increase luciferase levels when the TM K271R mutant of FoxO3 was coexpressed (Fig. 7E), suggesting that methylation at K271 is necessary for the activation of FoxO3 mediated transcriptional activation.

Taken together, these studies indicate that FoxO3 is

methylated at lysine 271 by Set9, and that this modification does not affect FoxO3 subcellular localiza-

tion, but decreases FoxO3 protein stability while eliciting a modest increase in FoxO3 transcriptional activity.

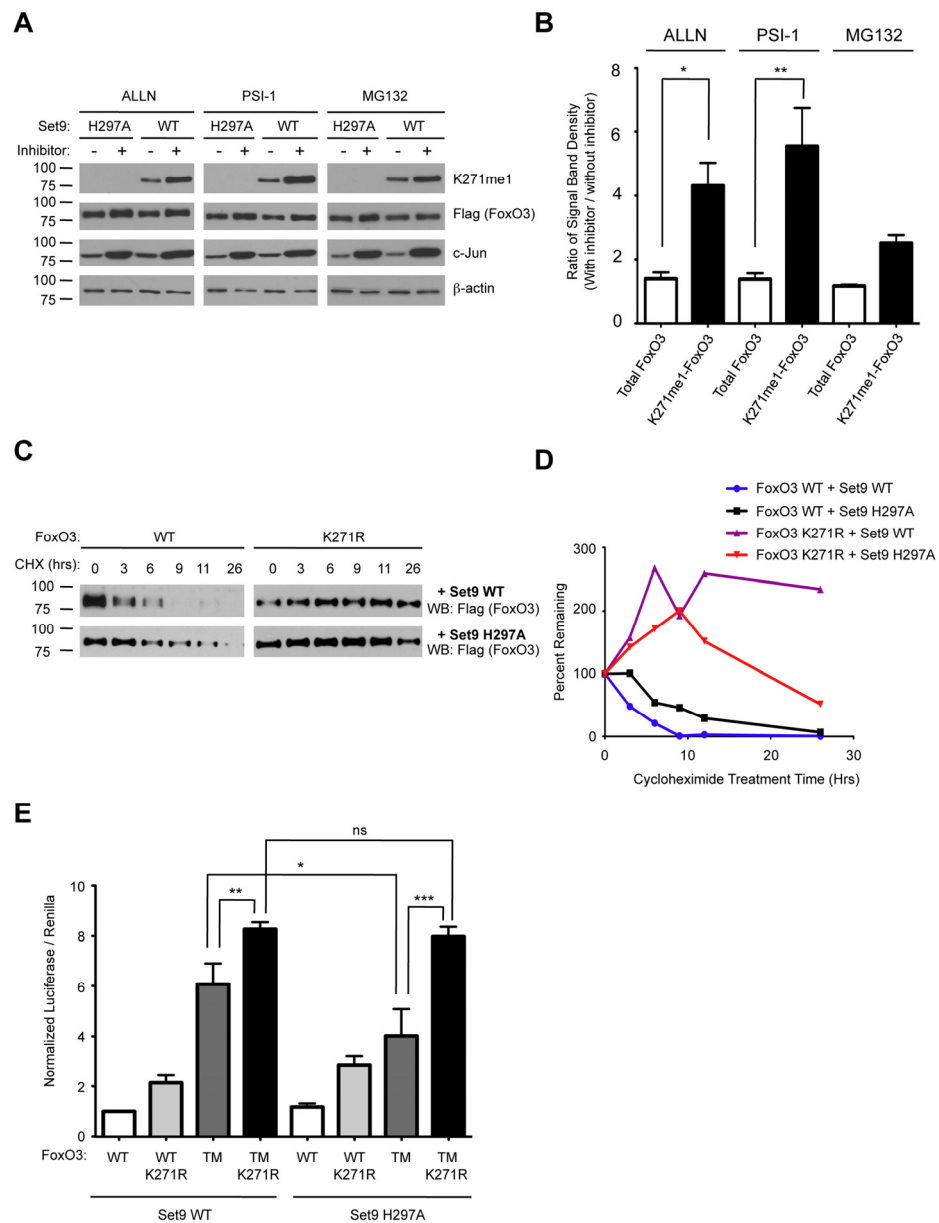


Figure 7. Methylation of FoxO3 at lysine 271 promotes FoxO3 degradation, while increasing FoxO3 transcriptional activity. (A) Methylated FoxO3 is less stable than the unmethylated form. 293T cells were co-transfected with Flag-FoxO3 and Flag-Set9 (WT or H297A). The cells were then treated with MG132 (20 μ M), ALLN (40 μ M) or PSI1 (40 μ M) for 16 hours prior to lysis. Extracts were analyzed by western-blot with antibodies to K271me1, Flag, c-Jun, and b-actin. (B) Western-blots from (A) were analyzed by densitometry and the ratio of intensity in the presence or absence of proteasome inhibitor was compared after normalization to b-actin. * $p < 0.05$, ** $p < 0.01$, One way ANOVA, Bonferroni post test. (C) K271R is more stable than wild type FoxO3. 293T cells were transfected with Flag-FoxO3 (WT or K271R) together with Flag-Set9 (WT or H297A). Cells were treated for the indicated length of time with 20 μ M cycloheximide (CHX) and FoxO3 expression was tested by western-blot with antibodies to Flag. (D) Western-blots from (C) were analyzed by densitometry at each time point of cycloheximide treatment. Results were normalized to the untreated well for each condition. (E) Set9 increases the transcriptional activity of the constitutively nuclear form of FoxO3. Flag-Set9 (WT or H297A) was co-expressed with Flag-FoxO3 (WT, K271R, TM [T32A/S253A/S315A], or TM K271R [T32A/S253A/K271R/S315A]) in 293T cells together with a 6xDBE-luciferase reporter construct, and luciferase activity was measured. The data represents the mean and SEM from 5 independent experiments, conducted in triplicate. All samples were normalized to the Flag-FoxO3 WT + Flag-Set9 WT condition. * $p < 0.05$, ** $p < 0.01$, *** $p < 0.001$, ns: $p > 0.05$, One way ANOVA, Bonferroni post test.

DISCUSSION

Lysine methylation of non-histone proteins has been recently found to be critical for a number of cellular responses, including the response to stress stimuli [68, 69, 72, 74]. In several cases, methylation affects the status of other post-translational modifications (PTMs) present on the target protein [72]. Lysine 271, the Set9 methylation site on FoxO3 has been previously shown to be acetylated [54]. Thus, methylation at FoxO3 lysine 271 could block acetylation at this site. It is possible that the competition for modifying lysine 271 could partly control FoxO3-dependent responses to stress stimuli. Like other PTMs, FoxO3 K271 methylation might be regulated by external stimuli. Indeed, we have found that oxidative stress can change the level of FoxO3 K271 methylation under certain conditions (data not shown). It is possible that the activity of protein deacetylases, such as Sirt1, which can deacetylate K271 (A.B., unpublished data), could facilitate methylation at this residue and therefore act in partnership with Set9 to regulate the presence of the methylated form of FoxO3 at the chromatin and increase FoxO3 transcriptional activity.

The conservation of lysine 271 and the residues surrounding this lysine in all FoxO family members, and yet the absence of significant methylation of FoxO1, FoxO4, and FoxO6 by Set9 indicates that the mechanism of target identification by Set9 could be more complex than a simple consensus sequence. Comparison of the known Set9 targets does not display a clear consensus for residues surrounding the lysine residue that is methylated. All of the targets have at least one positively charged residue N- or C-terminal to the site of methylation, so the active site of Set9 could require a local positive charge interaction for methylation or the positively charged residue could be important for hydrogen bonding with a residue in Set9. This was shown to be the case for p53 [69]. In addition, all of the substrates have a negatively charged residue at position +4 or +5 compared to the methylation site, and this negative charge could be important in positioning the substrate for methylation. However, given the lack of a strong consensus sequence, it is probable that the substrates of Set9 need to have a secondary structure that is not immediately identifiable from the amino acid sequence. The Set9 crystal structure with a p53 peptide was found to be similar to that of the Set9 crystal structure with a mono-methyl H3 peptide [69, 76]. The necessity of the lysine side chain of the residue to be methylated to enter a narrow channel in order to access the methyl-donor cofactor illustrates how important secondary structure of the substrate is for Set9 activity. It is possible that the substrate must have a flexible

secondary structure, much like a histone tail, in order to allow the lysine side chain access to this channel within Set9.

The regulation of FoxO3 activity by methylation could be pivotal to precisely modulate FoxO3's activity in response to stress. The increase in FoxO3 activity combined with a decrease in stability could create a transient pulse of FoxO3 activity intended to upregulate genes to mount an immediate response to stress. An increase in activity and decrease in stability has also been seen as a consequence of deacetylation on the FoxO family [59], consistent with a possible coordinated action of deacetylation and methylation. Mutations that increase the transcriptional activity of FoxO proteins without decreasing FoxO stability often lead to apoptosis (as is the case with the TM mutation). Thus, a transient pulse of FoxO activity may preferentially lead to the upregulation of stress resistance genes, without resulting in the upregulation of apoptosis genes.

Lysine methylation of FoxO3 represents a previously unidentified type of post-translational modification that adds to the growing number of PTMs on this transcription factor. Together, FoxO3 PTMs may form a 'code' for fine-tuning the activity of this transcription factor in cells. Interestingly, there seem to be interaction between the different FoxO3 PTMs. For example, arginine methylation of FoxO1 by PRMT1 has recently been described to inhibit the phosphorylation, and subsequent degradation, of FoxO1 by Akt [79]. Much like lysine methylation, arginine methylation can have a potent impact on the transcriptional activity of non-histone substrates [80]. It will be interesting to determine if lysine and arginine methylation both occur on the FoxO3 molecule and how they might interact with one another. The interaction between the different PTMs of FoxO3 at the same residue (e.g. acetylation/methylation/ubiquitination of a given lysine residue) or at different residues (e.g. lysine methylation versus arginine methylation) may alter several properties of the FoxO3 protein, including its stability, subcellular localization, recruitment to a subset of target genes, and interaction with protein partners.

Different PTMs might also serve to modulate FoxO3 activity differentially in different tissues and cellular environments. For example, a very recent study showed that Set9 also methylates FoxO3 at lysine 270, and that K270 methylation diminishes FoxO3's pro-apoptotic activity in neuronal cells by preventing FoxO3 binding to the promoter of the pro-apoptotic gene Bim [81]. This is in contrast with our study, since we find that methylation of FoxO3 at lysine 271 induces a modest

increase in FoxO3 transcriptional activity – as measured by reporter assay – in 293T cells. It will be interesting to compare how methylation at lysine 270 and 271 modulate FoxO3 activity, and whether their effects on FoxO3 function is dependent on the cell type or the type of target genes.

Together with published data, our results indicate that FoxO3, a transcription factor critical for stress resistance and longevity in a wide range of species, has evolved to be a heavily post-translationally regulated molecule, with about thirty different post-translationally modified residues described so far. FoxO3 appears to be a ‘hub’ in a network of genes regulating cellular homeostasis and energy metabolism. Thus, the variety and complexity of FoxO3 PTMs may be critical for the interface between extrinsic stimuli and intrinsic networks that regulate plastic phenotypes, including stem cell homeostasis, that ultimately contribute to organismal longevity.

EXPERIMENTAL PROCEDURES

Antibodies. The FoxO3 antibody (‘NFL’) was described previously [18]. The Flag and Set9 antibodies were obtained from Sigma and Cell Signaling Technologies, respectively. The H2B antibody was obtained from Millipore. The c-Jun, and β -actin and GFP (3E6 monoclonal) antibodies were purchased from Santa Cruz, Novus Biologicals and Invitrogen, respectively. The mono-methyl-specific antibody was generated by Quality Controlled Biochemicals. A branched mono-methylated peptide encompassing human FoxO3 K271 (Fig. 4A) was synthesized by the Keck Biotechnology Resource Laboratory at Yale University. This peptide was coupled to Keyhole limpet hemocyanin and injected into rabbits for antibody production. The serum was purified on a streptavidin column bound to a biotin conjugated linear mono-methyl peptide synthesized by the Keck Biotechnology Resource Laboratory.

Reagents. LY294002, ALLN and PSI-1 were all obtained from EMD Biosciences/Calbiochem. MG132 and Cycloheximide were purchased from Sigma.

Constructs. The constructs encoding GST-FoxO1, GST-FoxO3, GST-FoxO4, and GST-FoxO6 in the pGex vector were described previously [18, 82]. The constructs encoding His-Set9 (WT and H297A) in the pET-28b vector, and Flag-Set9 (WT and H297A) in the pcDNA vector were described previously [66]. The Dot1, Suv420h1, and Set8 constructs were described previously [83]. The SetD4, Smyd4, Smyd1, and NSD3 were generated as fusion proteins between GST and the full-length human proteins and expressed in insect cells

(X.S. and O.G.). The reporter construct 6xDBE-luciferase was described previously [84]. The constructs encoding WT FoxO3, the T32A/S253A/S315A (TM) mutant, and the K269R/K270R/K271R mutant in the pECE expression vector were described previously [18, 54, 77]. The construct encoding the constitutively active form of Akt (Akt CA) was described [18]. The FoxO3-GFP construct was described previously [15]. The FoxO3-GFP K271R mutant was generated using site-directed mutagenesis (Stratagene) using the forward primer GCGCAGCCAAGAAGAGGGCAGCCCTGCA GACAGC. The mutants of FoxO3 lysine residues were generated in the pECE vector using site directed mutagenesis (Stratagene) with the following primers: K269R:CGTGGCCGCGCAGCCAGGAAGAAGGCA GCCCTGC
K270R:GGCCGCGCAGCCAAGAGGAAGGCAGCC CTGCAG
K269R/K270R:GCCGTGGCCGCGCAGCCAGGAGG AAGGCAGCCCTGCAGACAGCC
K269R/K271R:GCCGTGGCCGCGCAGCCAGGAAG AGGGCAGCCCTGCAGACAGCC
K270R/K271R:CGTGGCCGCGCAGCCAAGAGGAG GGCAGCCCTGCAGACAGCC
shRNA oligonucleotides directed at human Set9 were designed with pSico Oligomaker v1.5 (<http://web.mit.edu/jacks-lab/protocols/pSico.html>).
shRNA Set9 F:
TGAACCTTGTTCACGGAGAATTCAAGAGATTCT CCGTGAACAAAGTTCTTTTTC
shRNA Set9 R:
TCGAGAAAAAAAGAACCTTGTTCACGGAGAACATC TCTTGAATTCTCCGTGAACAAAGTTCA
These oligonucleotides were annealed and cloned into pSicoR (PSR) between the HpaI and Xho1 sites according and annealed as described (<http://web.mit.edu/jacks-lab/protocols/pSico.html>).

Protein purification. His-Set9 WT and H297A were purified using TALON Metal Affinity Resin according to the protocol provided by the manufacturer (BD Biosciences Clontech). GST fusion proteins were purified on Glutathione agarose beads (Sigma), according to the manufacturer’s protocol.

Cell culture - HEK293T, U87, and NIH3T3 cells were maintained in Dulbecco Modified Eagle Medium (DMEM, Invitrogen) supplemented with 10% Fetal Bovine Serum (FBS, Invitrogen) and 1% Penicillin/Streptomycin/Glutamine (P/S/Q, Invitrogen). When indicated, cells were serum-starved by washing once with DMEM + 1% P/S/Q and then incubating them overnight in DMEM + 1% P/S/Q. Cells were then treated with the PI3K inhibitor LY294002 (EMD Biosciences, 20 μ M) for 2 hours prior to lysing.

Luciferase Assays. 293T cells were seeded at the density of 1.25×10^5 cells per well in 24 well plates. In each well, 250 ng of the appropriate FoxO3 constructs and 50 ng of the Set9 constructs were co-transfected with 250 ng of the 6xDBE luciferase reporter construct [84] and 50 ng of the Renilla control construct using TransIT-293 (Mirus, 2 μ l per well). Twenty-four hours after transfection, cells were lysed in 100 μ l of 1x passive lysis buffer (Promega). After centrifugation to remove cellular debris, the luminescence was measured in a Wallac Victor2 multilabel counter using the Dual-Luciferase reporter assay system (Promega), according to the manufacturer's protocol.

In Vitro Methylation Assay. *In vitro* methylation assays were conducted in a total volume of 25 μ l using 2 μ g of substrate, 100 ng of Set9 WT or H297A, in the methylation buffer: 150 mM NaCl, 20mM Tris-HCl [pH 7.5], 1 mM EDTA, 0.02% Triton. Depending on the reaction, either 40 μ M S-Adenosyl methionine (SAM, Sigma) or 300 nM S-[methyl-3H] Adenosyl-L-Methionine (Perkin Elmer, 0.55 μ Ci per reaction) was added. Reactions were carried out at 37°C for 3 hours to overnight. The reaction was resolved by SDS-PAGE (10%). After electrophoresis the gel was incubated with EN3HANCE™ Autoradiography Enhancer (Perkin Elmer cat#6NE9701) as directed by the supplier. The gel was then dried and autoradiographed at -80°C in a BioMax TranScreen LE Intensifying Screen along with Kodak "Biomax" MS film.

Generation of Stable Cell Lines. 293T cells were seeded at 3.5×10^6 cells per 10 cm plate and transfected with 10 μ g of the shRNA PSR constructs together with 5 μ g of the VSVg and 5 μ g of the Δ 8.2 helper plasmids [85] using a calcium phosphate procedure. The medium was changed 12 hours after transfection. 293T cells (2.5×10^6 cells/ml in 10 cm plates) were infected by 0.45 μ m-filtered supernatant from virus-producing cells in the presence of 8 μ g/ml polybrene. The cells were infected 3 times every 24 hours. After the third infection, the cells were seeded at a density of 2.5×10^6 cells per 10 cm plate and treated with 7 μ g/ml of puromycin. After 3 days, the puromycin resistant cells were maintained with 5 μ g/ml puromycin.

Western-Blot Analysis. Protein lysates for western-blots were prepared in two different ways. Cells from a 10 cm plate were lysed in 500 μ l of Triton lysis buffer (50 mM Tris-HCl [pH 7.5], 100 mM NaCl, 0.5 mM EDTA, 0.4% Triton, 50 mM NaF, 40 mM β -glycerophosphate, 1 mM sodium orthovanadate, 1 mM PMSF, 0.055 units/ml aprotinin). Cell extracts were collected and

centrifuged at 16,000 g for 10 min. Supernatant was collected and boiled in Laemmli sample buffer (2% SDS, 10% glycerol, 5% b-mercaptoethanol, 63 mM Tris-HCl [pH 6.8], 0.0025% bromophenol blue) at 95°C for 1 min. Alternatively, to ensure chromatin and membrane bound proteins were collected, cells were lysed in RIPA buffer (50 mM Tris-HCl [pH 7.5], 150 mM NaCl, 20 mM EDTA, 1% NP-40, 0.1% SDS, 1 mM PMSF, EDTA-free protease inhibitor cocktail [Roche]). Collected extracts were sonicated for 45 s on a VirTris Virsonic Digital 600 at 6W, and then centrifuged at 16,000 g for 10 min. The supernatant was incubated at 70°C for 10 min in Laemmli sample buffer. Extracts were resolved on a by SDS PAGE (10%) and transferred to nitrocellulose membranes. The membranes were incubated with primary antibodies (K271me1, 1:500; FoxO3 NFL, 1:500; Flag, 1:2000; b-actin, 1:5000; Set9, 1:2000; H2B, 1:5000), and the primary antibodies were visualized using horseradish peroxidase-conjugated secondary antibody (Calbiochem) and ECL Western-Blot Detection Reagent (Amersham Biosciences).

Cell Fractionation. Small-scale fractionation was carried out as described previously [86]. Briefly, the cytoplasmic fraction was collected by incubating scraped cells in Buffer A (10 mM HEPES [pH 7.9], 10 mM KCl, 1.5 mM MgCl₂, 0.34 M Sucrose, 10 % Glycerol, 1 mM DTT, 0.1% Triton-X-100, EDTA-free protease inhibitor cocktail [Roche]) for 10 min, and nuclei were separated by centrifugation at 1,300 g for 5 min. The nuclei were then lysed in Buffer B (3 mM EDTA, 0.2 mM EGTA, 1 mM DTT, EDTA-free protease inhibitor cocktail [Roche]) for 30 min on ice. Chromatin and other insoluble cell parts were separated from nucleoplasm fraction by centrifugation at 1,700 g for 5 min. All fractions were incubated at 70°C for 10 min in Laemmli sample buffer. The chromatin fraction was sonicated in Laemmli sample buffer for 30 s at 6W. Different fractions were analyzed by western-blot as described above.

Scoring of FoxO3 Subcellular Localization in U87 Cells
U87 cells were plated in 12 well plates on glass coverslips at a density of 3×10^5 cells per well. The cells were transfected using TransIT-293 (Mirus, 4 μ l per well) according to the supplier's protocol. For each transfection, 0.8 μ g of FoxO3-GFP plasmid and 0.4 μ g of Set9 plasmid was used. Cells were fixed 2 days post transfection with 4% paraformaldehyde (PFA) for 15 minutes. They were then washed 5 times with 1x PBS. Coverslips were mounted using Vectashield Hard Set with Dapi (Vector Laboratories) and examined under a Zeiss Axioskop2 Plus with a FLuoArc Ultraviolet module. Counting of FoxO3-GFP subcellular

localization was done in a blinded manner and a minimum of 200 cells were counted per condition for each experiment. If the outline of the nucleus was clearly visible in the GFP channel, FoxO3 localization was scored as cytoplasmic. If the nucleus was clearly visible in the GFP channel, FoxO3 localization was scored as nuclear. If neither of these conditions were met, FoxO3 localization was scored as ubiquitous. Statistics were done on the percentage of cells in each condition over 3 independent experiments and significance was determined using a Bonferroni posttest.

Immunofluorescence in NIH3T3 cells. NIH3T3 cells were plated in 6 well plates on poly-L-lysine coated glass coverslips at a density of 106 cells/well. Cells were transfected with FoxO3-GFP or FoxO3-GFP K271R and Flag-Set9 WT or H297A at a ratio of 4 μ g:6 μ g Foxo:Set9 using Lipofectamine 2000 (Invitrogen, 10 μ l per well), according to the manufacturer's protocol. Cells were fixed 24 hours post-transfection with 4% PFA for 15 min. Cells were then washed 5 times with 1x PBS. Coverslips were blocked with PBS supplemented with 3% BSA and 0.1% Triton X-100 (PBS-BT) and stained with DAPI, mouse anti-GFP 3E6 monoclonal antibody (Invitrogen, 1:500), K271me1 polyclonal antibody (1:500) and appropriate secondary antibodies labeled with Alexa Fluor 488 (anti-mouse IgG) or 594 (anti-rabbit IgG), respectively (Invitrogen, 1:250). Coverslips were mounted using anti-fade mounting medium containing PBS, glycerol and P-phenylenediamine. Coverslips were imaged on an Axiovert 200M (Zeiss) equipped with a CCD camera (Hamamatsu c47429512ERG). Coverslips were imaged in a blinded manner. Contrast enhancement was performed using Photoshop CS3 (Adobe).

Tandem Mass Spectrometry Analysis. A Coomassie-stained band corresponding to GST-FoxO3 methylated by Set9 was excised from an SDS-polyacrylamide gel, divided in half, reduced with dithiothreitol, alkylated with iodoacetamide, and digested with either trypsin or chymotrypsin. Peptide mixtures were separated by microcapillary reverse-phase chromatography and analyzed online in a hybrid linear ion trap-Orbitrap (LTQ-Orbitrap; Thermo Electron) mass spectrometer [87]. Mass spectra were data base-searched using the SEQUEST algorithm. All peptide matches were initially filtered based on enzyme specificity, mass measurement error, XCorr and DCorr scores and further manually validated for peptide identification and site localization.

Generation of Protein Microarray, Peptide Synthesis, and Labeling. The generation of protein microarrays has been described [78]. Methylated and unmethylated

forms of the K271 biotinylated peptide were synthesized by the W. M. Keck Biotechnology Resource Center (New Haven, CT). Biotinylated peptides (10 μ g) were labeled as previously described [78]. A GenePix 4200A scanner (Axon, Inc.) was used for array analysis.

ACKNOWLEDGEMENTS

We thank members of the Brunet lab for critical comments and for reading the manuscript. This work was supported by an NIH R01 AG026648 to A.B., an NIH R01 GM079641 to O.G., a joint NIH R21 DA25800 to M.T.B and O.G., and by an NIH Ruth L. Kirschstein National Research Service Award 5T32 CA09302 to D.R.C., A.E.W. and T.R.S. D.R.C. and T.R.S. were also supported by an NIH Ruth L. Kirschstein National Research Service Award F31 NS059101 and by a NSF graduate fellowship, respectively.

CONFLICT OF INTERESTS STATEMENT

The authors of this manuscript have no conflict of interest to declare.

REFERENCES

1. Lin K, Dorman JB, Rodan A, Kenyon C. daf-16: An HNF-3/forkhead family member that can function to double the lifespan of *Caenorhabditis elegans*. *Science*. 1997; 278:1319-1322.
2. Ogg S, Paradis S, Gottlieb S, Patterson GI, Lee L, Tissenbaum HA, Ruvkun G. The Fork head transcription factor DAF-16 transduces insulin-like metabolic and longevity signals in *C. elegans*. *Nature*. 1997; 389:994-999.
3. Henderson ST, Johnson TE. daf-16 integrates developmental and environmental inputs to mediate aging in the nematode *Caenorhabditis elegans*. *Curr Biol*. 2001; 11:1975-1980.
4. Giannakou ME, Goss M, Junger MA, Hafen E, Leevers SJ, Partridge L. Long-lived *Drosophila* with overexpressed dFOXO in adult fat body. *Science*. 2004; 305:361.
5. Hwangbo DS, Gersham B, Tu MP, Palmer M, Tatar M. *Drosophila* dFOXO controls lifespan and regulates insulin signalling in brain and fat body. *Nature*. 2004; 429:562-566.
6. Holzenberger M, Dupont J, Ducos B, Leneuve P, Geloen A, Even PC, Cervera P, Le Bouc Y. IGF-1 receptor regulates lifespan and resistance to oxidative stress in mice. *Nature*. 2003; 421:182-187.
7. Bluher M, Kahn BB, Kahn CR. Extended longevity in mice lacking the insulin receptor in adipose tissue. *Science*. 2003; 299:572-574.
8. Willcox BJ, Donlon TA, He Q, Chen R, Grove JS, Yano K, Masaki KH, Willcox DC, Rodriguez B, Curb JD. FOXO3A genotype is strongly associated with human longevity. *Proc Natl Acad Sci U S A*. 2008; 105:13987-13992.
9. Anselmi CV, Malovini A, Roncarati R, Novelli V, Villa F, Condorelli G, Bellazzi R, Puca AA. Association of the FOXO3A

locus with extreme longevity in a southern Italian centenarian study. *Rejuvenation Res.* 2009; 12:95-104.

10. Flachsbart F, Caliebe A, Kleindorp R, Blanche H, von Eller-Eberstein H, Nikolaus S, Schreiber S, Nebel A. Association of FOXO3A variation with human longevity confirmed in German centenarians. *Proc Natl Acad Sci U S A.* 2009; 106:2700-2705.

11. Pawlikowska L, Hu D, Huntsman S, Sung A, Chu C, Chen J, Joyner AH, Schork NJ, Hsueh WC, Reiner AP, Psaty BM, Atzmon G, Barzilai N, et al. Association of common genetic variation in the insulin/IGF1 signaling pathway with human longevity. *Aging Cell.* 2009; 8:460-472.

12. Li Y, Wang WJ, Cao H, Lu J, Wu C, Hu FY, Guo J, Zhao L, Yang F, Zhang YX, Li W, Zheng GY, Cui H, et al. Genetic association of FOXO1A and FOXO3A with longevity trait in Han Chinese populations. *Hum Mol Genet.* 2009; 18:4897-4904.

13. Dansen TB, Burgering BM. Unravelling the tumor-suppressive functions of FOXO proteins. *Trends Cell Biol.* 2008; 18:421-429.

14. Paik JH, Kollipara R, Chu G, Ji H, Xiao Y, Ding Z, Miao L, Tothova Z, Horner JW, Carrasco DR, Jiang S, Gilliland DG, Chin L, et al. FoxOs are lineage-restricted redundant tumor suppressors and regulate endothelial cell homeostasis. *Cell.* 2007; 128:309-323.

15. Hu MC, Lee DF, Xia W, Golfman LS, Ou-Yang F, Yang JY, Zou Y, Bao S, Hanada N, Saso H, Kobayashi R, Hung MC. IkappaB kinase promotes tumorigenesis through inhibition of forkhead FOXO3a. *Cell.* 2004; 117:225-237.

16. Zou Y, Tsai WB, Cheng CJ, Hsu C, Chung YM, Li PC, Lin SH, Hu MC. Forkhead box transcription factor FOXO3a suppresses estrogen-dependent breast cancer cell proliferation and tumorigenesis. *Breast Cancer Res.* 2008; 10:R21.

17. Bakker WJ, Harris IS, Mak TW. FOXO3a is activated in response to hypoxic stress and inhibits HIF1-induced apoptosis via regulation of CITED2. *Mol Cell.* 2007; 28:941-953.

18. Brunet A, Bonni A, Zigmond MJ, Lin MZ, Juo P, Hu LS, Anderson MJ, Arden KC, Blenis J, Greenberg ME. Akt promotes cell survival by phosphorylating and inhibiting a Forkhead transcription factor. *Cell.* 1999; 96:857-868.

19. Dijkers PF, Medema RH, Pals C, Banerji L, Thomas NS, Lam EW, Burgering BM, Raaijmakers JA, Lammers JW, Koenderman L, Coffer PJ. Forkhead transcription factor FKHL-1 modulates cytokine-dependent transcriptional regulation of p27(KIP1). *Mol Cell Biol.* 2000; 20:9138-9148.

20. Medema RH, Kops GJ, Bos JL, Burgering BM. AFX-like Forkhead transcription factors mediate cell-cycle regulation by Ras and PKB through p27kip1. *Nature.* 2000; 404:782-787.

21. Kops GJ, Dansen TB, Polderman PE, Saarloos I, Wirtz KW, Coffer PJ, Huang TT, Bos JL, Medema RH, Burgering BM. Forkhead transcription factor FOXO3a protects quiescent cells from oxidative stress. *Nature.* 2002; 419:316-321.

22. Nemoto S, Finkel T. Redox regulation of forkhead proteins through a p66shc-dependent signaling pathway. *Science.* 2002; 295:2450-2452.

23. Tran H, Brunet A, Grenier JM, Datta SR, Fornace AJ, Jr., DiStefano PS, Chiang LW, Greenberg ME. DNA repair pathway stimulated by the forkhead transcription factor FOXO3a through the Gadd45 protein. *Science.* 2002; 296:530-534.

24. Mammucari C, Milan G, Romanello V, Masiero E, Rudolf R, Del Piccolo P, Burden SJ, Di Lisi R, Sandri C, Zhao J, Goldberg AL, Schiaffino S, Sandri M. FoxO3 controls autophagy in skeletal muscle *in vivo*. *Cell Metab.* 2007; 6:458-471.

25. Zhao J, Brault JJ, Schild A, Cao P, Sandri M, Schiaffino S, Lecker SH, Goldberg AL. FoxO3 coordinately activates protein degradation by the autophagic/lysosomal and proteasomal pathways in atrophying muscle cells. *Cell Metab.* 2007; 6:472-483.

26. Lehtinen MK, Yuan Z, Boag PR, Yang Y, Villen J, Becker EB, DiBacco S, de la Iglesia N, Gygi S, Blackwell TK, Bonni A. A conserved MST-FOXO signaling pathway mediates oxidative-stress responses and extends life span. *Cell.* 2006; 125:987-1001.

27. Matsumoto M, Han S, Kitamura T, Accili D. Dual role of transcription factor FoxO1 in controlling hepatic insulin sensitivity and lipid metabolism. *J Clin Invest.* 2006; 116:2464-2472.

28. Kitamura T, Feng Y, Kitamura YI, Chua SC, Jr., Xu AW, Barsh GS, Rossetti L, Accili D. Forkhead protein FoxO1 mediates AgRP-dependent effects of leptin on food intake. *Nat Med.* 2006; 12:534-540.

29. Hribal ML, Nakae J, Kitamura T, Shutter JR, Accili D. Regulation of insulin-like growth factor-dependent myoblast differentiation by Foxo forkhead transcription factors. *J Cell Biol.* 2003; 162:535-541.

30. Nakae J, Kitamura T, Kitamura Y, Biggs WH, 3rd, Arden KC, Accili D. The forkhead transcription factor Foxo1 regulates adipocyte differentiation. *Dev Cell.* 2003; 4:119-129.

31. Renault VM, Rafalski VA, Morgan AA, Salih DA, Brett JO, Webb AE, Villeda SA, Thekkat PU, Guillerey C, Denko NC, Palmer TD, Butte AJ, Brunet A. FoxO3 regulates neural stem cell homeostasis. *Cell Stem Cell.* 2009; 5:527-539.

32. Tothova Z, Kollipara R, Huntly BJ, Lee BH, Castrillon DH, Cullen DE, McDowell EP, Lazo-Kallanian S, Williams IR, Sears C, Armstrong SA, Passegue E, DePinho RA, et al. FoxOs are critical mediators of hematopoietic stem cell resistance to physiologic oxidative stress. *Cell.* 2007; 128:325-339.

33. Paik JH, Ding Z, Narurkar R, Ramkissoon S, Muller F, Kamoun WS, Chae SS, Zheng H, Ying H, Mahoney J, Hiller D, Jiang S, Protopopov A, et al. FoxOs cooperatively regulate diverse pathways governing neural stem cell homeostasis. *Cell Stem Cell.* 2009; 5:540-553.

34. Miyamoto K, Araki KY, Naka K, Arai F, Takubo K, Yamazaki S, Matsuoka S, Miyamoto T, Ito K, Ohmura M, Chen C, Hosokawa K, Nakuchi H, et al. Foxo3a is essential for maintenance of the hematopoietic stem cell pool. *Cell Stem Cell.* 2007; 1:101-112.

35. Miyamoto K, Miyamoto T, Kato R, Yoshimura A, Motoyama N, Suda T. FoxO3a regulates hematopoietic homeostasis through a negative feedback pathway in conditions of stress or aging. *Blood.* 2008; 112:4485-4493.

36. Greer EL, Brunet A. FOXO transcription factors in ageing and cancer. *Acta Physiol (Oxf).* 2008; 192:19-28.

37. Shin I, Bakin AV, Rodeck U, Brunet A, Arteaga CL. Transforming growth factor beta enhances epithelial cell survival via Akt-dependent regulation of FKHL1. *Mol Biol Cell.* 2001; 12:3328-3339.

38. Thepot S, Lainey E, Cluzeau T, Sebert M, Leroy C, Ades L, Tailler M, Galluzzi L, Baran-Marszak F, Roudot H, Eclache V, Gardin C, de Botton S, et al. Hypomethylating agents reactivate FOXO3A in acute myeloid leukemia. *Cell Cycle.* 2011; 10:2323-2330.

39. Brunet A, Park J, Tran H, Hu LS, Hemmings BA, Greenberg ME. Protein kinase SGK mediates survival signals by phosphorylating the forkhead transcription factor FKHL1 (FOXO3a). *Mol Cell Biol.* 2001; 21:952-965.

40. Biggs WHI, Meisenhelder J, Hunter T, Cavenee WK, Arden KC. Protein kinase B/Akt-mediated phosphorylation promotes nuclear exclusion of the winged helix transcription factor FKHR1. *Proc Natl Acad Sci USA*. 1999; 96:7421-7426.

41. Kops GJ, de Ruiter ND, De Vries-Smits AM, Powell DR, Bos JL, Burgering BM. Direct control of the Forkhead transcription factor AFX by protein kinase B. *Nature*. 1999; 398:630-634.

42. Nakae J, Park BC, Accili D. Insulin Stimulates Phosphorylation of the Forkhead Transcription Factor FKHR on Serine 253 through a Wortmannin-sensitive Pathway. *J Biol Chem*. 1999; 274:15982-15985.

43. Matsuzaki H, Daitoku H, Hatta M, Tanaka K, Fukamizu A. Insulin-induced phosphorylation of FKHR (Foxo1) targets to proteasomal degradation. *Proc Natl Acad Sci U S A*. 2003; 100:11285-11290.

44. Plas DR, Thompson CB. Akt activation promotes degradation of tuberin and FOXO3a via the proteasome. *J Biol Chem*. 2003; 278:12361-12366.

45. Aoki M, Jiang H, Vogt PK. Proteasomal degradation of the FoxO1 transcriptional regulator in cells transformed by the P3k and Akt oncoproteins. *Proc Natl Acad Sci U S A*. 2004; 101:13613-13617.

46. Huang H, Regan KM, Wang F, Wang D, Smith DL, van Deursen JM, Tindall DJ. Skp2 inhibits FOXO1 in tumor suppression through ubiquitin-mediated degradation. *Proc Natl Acad Sci U S A*. 2005; 102:1649-1654.

47. Yang JY, Zong CS, Xia W, Yamaguchi H, Ding Q, Xie X, Lang JY, Lai CC, Chang CJ, Huang WC, Huang H, Kuo HP, Lee DF, et al. ERK promotes tumorigenesis by inhibiting FOXO3a via MDM2-mediated degradation. *Nat Cell Biol*. 2008; 10:138-148.

48. Wang F, Chan CH, Chen K, Guan X, Lin HK, Tong Q. Deacetylation of FOXO3 by SIRT1 or SIRT2 leads to Skp2-mediated FOXO3 ubiquitination and degradation. *Oncogene*. 2012; 31:1546-1557.

49. van der Horst A, de Vries-Smits AM, Brenkman AB, van Triest MH, van den Broek N, Colland F, Maurice MM, Burgering BM. FOXO4 transcriptional activity is regulated by monoubiquitination and USP7/HAUSP. *Nat Cell Biol*. 2006; 8:1064-1073.

50. Brenkman AB, de Keizer PL, van den Broek NJ, Jochemsen AG, Burgering BM. Mdm2 induces mono-ubiquitination of FOXO4. *PLoS One*. 2008; 3:e2819.

51. Matsuzaki H, Daitoku H, Hatta M, Aoyama H, Yoshimochi K, Fukamizu A. Acetylation of Foxo1 alters its DNA-binding ability and sensitivity to phosphorylation. *Proc Natl Acad Sci U S A*. 2005; 102:11278-11283.

52. Tsai KL, Sun YJ, Huang CY, Yang JY, Hung MC, Hsiao CD. Crystal structure of the human FOXO3a-DBD/DNA complex suggests the effects of post-translational modification. *Nucleic Acids Res*. 2007; 35:6984-6994.

53. Fukuoka M, Daitoku H, Hatta M, Matsuzaki H, Umemura S, Fukamizu A. Negative regulation of forkhead transcription factor AFX (Foxo4) by CBP-induced acetylation. *Int J Mol Med*. 2003; 12:503-508.

54. Brunet A, Sweeney LB, Sturgill JF, Chua KF, Greer PL, Lin Y, Tran H, Ross SE, Mostoslavsky R, Cohen HY, Hu LS, Cheng HL, Jedrychowski MP, et al. Stress-dependent regulation of FOXO transcription factors by the SIRT1 deacetylase. *Science*. 2004; 303:2011-2015.

55. Daitoku H, Hatta M, Matsuzaki H, Aratani S, Ohshima T, Miyagishi M, Nakajima T, Fukamizu A. Silent information regulator 2 potentiates Foxo1-mediated transcription through its deacetylase activity. *Proc Natl Acad Sci U S A*. 2004; 101:10042-10047.

56. Motta MC, Divecha N, Lemieux M, Kamel C, Chen D, Gu W, Bultsma Y, McBurney M, Guarente L. Mammalian SIRT1 represses forkhead transcription factors. *Cell*. 2004; 116:551-563.

57. Van Der Horst A, Tertoolen LG, De Vries-Smits LM, Frye RA, Medema RH, Burgering BM. FOXO4 is acetylated upon peroxide stress and deacetylated by the longevity protein hSir2SIRT1. *J Biol Chem*. 2004.

58. Wang F, Nguyen M, Qin FX, Tong Q. SIRT2 deacetylates FOXO3a in response to oxidative stress and caloric restriction. *Aging Cell*. 2007; 6:505-514.

59. Kitamura YI, Kitamura T, Kruse JP, Raum JC, Stein R, Gu W, Accili D. FoxO1 protects against pancreatic beta cell failure through NeuroD and MafA induction. *Cell Metab*. 2005; 2:153-163.

60. Dansen TB, Smits LM, van Triest MH, de Keizer PL, van Leenen D, Koerkamp MG, Szypowska A, Meppelink A, Brenkman AB, Yodoi J, Holstege FC, Burgering BM. Redox-sensitive cysteines bridge p300/CBP-mediated acetylation and FoxO4 activity. *Nat Chem Biol*. 2009; 5:664-672.

61. Frescas D, Valenti L, Accili D. Nuclear trapping of the forkhead transcription factor FoxO1 via Sirt-dependent deacetylation promotes expression of glucogenetic genes. *J Biol Chem*. 2005; 280:20589-20595.

62. Calnan DR, Brunet A. The FoxO code. *Oncogene*. 2008; 27:2276-2288.

63. Berger SL. The complex language of chromatin regulation during transcription. *Nature*. 2007; 447:407-412.

64. Lan F, Shi Y. Epigenetic regulation: methylation of histone and non-histone proteins. *Sci China C Life Sci*. 2009; 52:311-322.

65. Allis CD, Berger SL, Cote J, Dent S, Jenuwien T, Kouzarides T, Pillus L, Reinberg D, Shi Y, Shiekhattar R, Shilatifard A, Workman J, Zhang Y. New nomenclature for chromatin-modifying enzymes. *Cell*. 2007; 131:633-636.

66. Nishioka K, Chuikov S, Sarma K, Erdjument-Bromage H, Allis CD, Tempst P, Reinberg D. Set9, a novel histone H3 methyltransferase that facilitates transcription by precluding histone tail modifications required for heterochromatin formation. *Genes Dev*. 2002; 16:479-489.

67. Esteve PO, Chin HG, Benner J, Feehery GR, Samaranayake M, Horwitz GA, Jacobsen SE, Pradhan S. Regulation of DNMT1 stability through SET7-mediated lysine methylation in mammalian cells. *Proc Natl Acad Sci U S A*. 2009; 106:5076-5081.

68. Yang XD, Huang B, Li M, Lamb A, Kelleher NL, Chen LF. Negative regulation of NF- κ B action by Set9-mediated lysine methylation of the RelA subunit. *Embo J*. 2009; 28:1055-1066.

69. Chuikov S, Kurash JK, Wilson JR, Xiao B, Justin N, Ivanov GS, McKinney K, Tempst P, Prives C, Gamblin SJ, Barlev NA, Reinberg D. Regulation of p53 activity through lysine methylation. *Nature*. 2004; 432:353-360.

70. Masatsugu T, Yamamoto K. Multiple lysine methylation of PCAF by Set9 methyltransferase. *Biochem Biophys Res Commun*. 2009; 381:22-26.

71. Kouskouti A, Scheer E, Staub A, Tora L, Talianidis I. Gene-specific modulation of TAF10 function by SET9-mediated methylation. *Mol Cell*. 2004; 14:175-182.

72. Ea CK, Baltimore D. Regulation of NF- κ B activity through lysine monomethylation of p65. *Proc Natl Acad Sci U S A*. 2009; 106:18972-18977.

73. Subramanian K, Jia D, Kapoor-Vazirani P, Powell DR, Collins RE, Sharma D, Peng J, Cheng X, Vertino PM. Regulation of estrogen receptor alpha by the SET7 lysine methyltransferase. *Mol Cell*. 2008; 30:336-347.

74. Ivanov GS, Ivanova T, Kurash J, Ivanov A, Chuikov S, Gizatullin F, Herrera-Medina EM, Rauscher F, 3rd, Reinberg D, Barlev NA. Methylation-acetylation interplay activates p53 in response to DNA damage. *Mol Cell Biol*. 2007; 27:6756-6769.

75. Kurash JK, Lei H, Shen Q, Marston WL, Granda BW, Fan H, Wall D, Li E, Gaudet F. Methylation of p53 by Set7/9 mediates p53 acetylation and activity *in vivo*. *Mol Cell*. 2008; 29:392-400.

76. Xiao B, Jing C, Wilson JR, Walker PA, Vasisht N, Kelly G, Howell S, Taylor IA, Blackburn GM, Gamblin SJ. Structure and catalytic mechanism of the human histone methyltransferase SET7/9. *Nature*. 2003; 421:652-656.

77. Brunet A, Kanai F, Stehn J, Xu J, Sarbassova D, Frangioni JV, Dalal SN, DeCaprio JA, Greenberg ME, Yaffe MB. 14-3-3 transits to the nucleus and participates in dynamic nucleocytoplasmic transport. *J Cell Biol*. 2002; 156:817-828.

78. Espejo A, Cote J, Bednarek A, Richard S, Bedford MT. A protein-domain microarray identifies novel protein-protein interactions. *Biochem J*. 2002; 367:697-702.

79. Yamagata K, Daitoku H, Takahashi Y, Namiki K, Hisatake K, Kako K, Mukai H, Kasuya Y, Fukamizu A. Arginine methylation of FOXO transcription factors inhibits their phosphorylation by Akt. *Mol Cell*. 2008; 32:221-231.

80. Lee YH, Stallcup MR. Minireview: protein arginine methylation of nonhistone proteins in transcriptional regulation. *Mol Endocrinol*. 2009; 23:425-433.

81. Xie Q, Hao Y, Tao L, Peng S, Rao C, Chen H, You H, Dong MQ, Yuan Z. Lysine methylation of FOXO3 regulates oxidative stress-induced neuronal cell death. *EMBO Rep*. 2012; 13:371-377.

82. Greer EL, Oskouie PR, Banko MR, Maniar JM, Gygi MP, Gygi SP, Brunet A. The energy sensor AMP-activated protein kinase directly regulates the mammalian FOXO3 transcription factor. *J Biol Chem*. 2007; 282:30107-30119.

83. Shi X, Kachirskaia I, Yamaguchi H, West LE, Wen H, Wang EW, Dutta S, Appella E, Gozani O. Modulation of p53 function by SET8-mediated methylation at lysine 382. *Mol Cell*. 2007; 27:636-646.

84. Furuyama T, Kitayama K, Yamashita H, Mori N. Forkhead transcription factor FOXO1 (FKHR)-dependent induction of PDK4 gene expression in skeletal muscle during energy deprivation. *Biochem J*. 2003; 375:365-371.

85. Ventura A, Meissner A, Dillon CP, McManus M, Sharp PA, Van Parijs L, Jaenisch R, Jacks T. Cre-lox-regulated conditional RNA interference from transgenes. *Proc Natl Acad Sci U S A*. 2004; 101:10380-10385.

86. Mendez J, Stillman B. Chromatin association of human origin recognition complex, cdc6, and minichromosome maintenance proteins during the cell cycle: assembly of prereplication complexes in late mitosis. *Mol Cell Biol*. 2000; 20:8602-8612.

87. Haas W, Faherty BK, Gerber SA, Elias JE, Beausoleil SA, Bakalarski CE, Li X, Villen J, Gygi SP. Optimization and use of peptide mass measurement accuracy in shotgun proteomics. *Mol Cell Proteomics*. 2006; 5:1326-1337.